Journal of Adhesion Science and Technology
Publication details, including instructions for authors and subscription information:
http://www.tandfonline.com/loi/tast20

An experimental study on the dependence of the strength of adhesively bonded joints with thickness and mechanical properties of the adhesives

Sen Yang[a], Wei Xu[ab], Lihong Liang[a], Tzuchiang Wang[a] & Yueguang Wei[a]

[a] State Key Laboratory of Nonlinear Mechanics, Institute of Mechanics, Chinese Academy of Sciences, Beijing 100190, P.R. China

[b] Beijing Key Laboratory of Aeronautical Materials Testing and Evaluation, Laboratory of Science and Technology on Advanced High Temperature Structure Materials, Beijing Institute of Aeronautical Materials, Beijing 100095, P.R. China

Published online: 24 Feb 2014.

To cite this article: Sen Yang, Wei Xu, Lihong Liang, Tzuchiang Wang & Yueguang Wei (2014) An experimental study on the dependence of the strength of adhesively bonded joints with thickness and mechanical properties of the adhesives, Journal of Adhesion Science and Technology, 28:11, 1055-1071, DOI: 10.1080/01694243.2014.884753

To link to this article: http://dx.doi.org/10.1080/01694243.2014.884753

Journal of Adhesion Science and Technology, 2014
Vol. 28, No. 11, 1055–1071, http://dx.doi.org/10.1080/01694243.2014.884753

Taylor & Francis
Taylor & Francis Group

An experimental study on the dependence of the strength of adhesively bonded joints with thickness and mechanical properties of the adhesives

Sen Yang[a], Wei Xu[a,b]*, Lihong Liang[a], Tzuchiang Wang[a] and Yueguang Wei[a]*

[a]*State Key Laboratory of Nonlinear Mechanics, Institute of Mechanics, Chinese Academy of Sciences, Beijing 100190, P.R. China;* [b]*Beijing Key Laboratory of Aeronautical Materials Testing and Evaluation, Laboratory of Science and Technology on Advanced High Temperature Structure Materials, Beijing Institute of Aeronautical Materials, Beijing 100095, P.R. China*

(*Received 8 May 2013; final version received 22 December 2013; accepted 14 January 2014*)

Adhesive bonding joints are widely applied in many engineering fields. Their overall strength is much dependent on the thickness of adhesive layers. Many previous experimental studies have found that the ultimate failure strength of the bonding structure increases with the decrease of the adhesive thickness. However, few of them consider the effect of adhesive intrinsic material parameters on the relation between the overall strength and adhesive thickness. In the present investigation, the effect of the adhesive thickness on the overall strength of the lightweight metallic adhesive bonding joints was experimentally studied, considering the effect of the adhesive toughness. The results show that the variations of overall strength resulting from the adhesive thicknesses have remarkable discrepancy due to the toughness of the adhesive, which is in agreement with the previous model prediction.

Keywords: adhesive thickness; toughness; bulk shear strength of adhesive; overall strength

1. Introduction

Adhesive bonding joints are being widely used to connect dissimilar materials in various industries including civil engineering, automotive, and aeronautic industries because the adhesive structures are economical, easy to prepare, and especially lightweight. With the continuous emergence of novel polymer-based adhesives, the application of the adhesive bonding structures would be wider. The study for the mechanical properties of adhesive bonding structures is really significant and attractive, and thus many researchers [1–9] have focused their research on the different aspects of joints, such as failure strength,[1–3,5,8] critical energy release,[4,7,9] and cohesive parameters of joints.[6] The overall strength of the joints significantly depends on the adhesive properties, which are characterized by the strength and energy rate mixities of the adhesive.[1] Some external factors also affect the failure strength of joints such as temperature,[3] filler content in adhesive,[5] slip, and rotation angle [8]; especially, the overall strength of the adhesive joints is a key issue. Therefore, some theoretical and computational models to predict the failure have been proposed,[10] considering some systemic

*Corresponding authors. Emails: xuwei@lnm.imech.ac.cn (W. Xu); ywei@lnm.imech.ac.cn (Y. Wei)

parameters of the adhesive joints, such as material properties and geometrical parameters. Among them, adhesive thickness is one of the most significant parameter and is worth studying.

Recently, the researches based on the experiments have shown that the overall strength is influenced substantially by adhesive thickness. The high-strength steel single-lap joints (SLJ) bonded by various types of epoxy-based adhesives layers were investigated by da Silva and his co-workers.[11,12] The experiment results showed that the failure strength increases as the adhesive thickness gets thinner. Other researches also point out similar conclusion with different adhesives for SLJ. Furthermore, some other types of bonding structure have also been investigated. The interfacial strength of the double cantilever beam increases with decreasing adhesive thickness. Chai et al. [3] carried out the experimental research for adhesive thickness effect using the Napkin Ring specimen. They found that both ultimate shear strength and strain increase monotonically with decreasing adhesive thickness. Lee et al. [13] investigated the effect of bond thickness on the fracture toughness of compact tension adhesive joint specimens, which showed that fracture toughness decreased with increasing bond thickness, and tending to be a stable value at larger thickness. Similarly, tubular butt joint could be also regarded as pure tensile specimen adopted by Castagnetti et al. [14] to study the influence of bonding thickness; the result was found to be similar to the other tests mentioned above.

Some researchers established a variety of theories to explain this phenomenon.[13,15,16] Adams et al. [10] believed that thicker bond-lines contained more defects such as micro-cracks and voids so that the failure load increases as the adhesive thickness gets thinner. Some other explanation for the effect of the adhesive thickness was established by Gleich et al. [15], who utilized the finite element simulation to study the effect of adhesive thickness. He found that both peel and shear interface stress between the adherend and the adhesive tended to increase as the adhesive thickness got thinner. A failure criterion based on the interface stresses can explain the effect of adhesive thickness if the failure occurs close to the adhesive–adherend interface. Lee et al. [13] gave some explanation. The interfaces between the adhesive and the adherends had a stronger constraint effect for the thinner adhesive thickness compact tension sample. Pardon et al. [16] applied the cohesive zone models to explain the thickness effect due to the internal and external constraint. From internal point of view, as long as the adhesive thickness is thin enough, the adhesive layer will be fully plastic deformation. Then, the height of the plastic zone will be equal to adhesive thickness. Furthermore, they pointed out that the material properties of the adhesive had a remarkable effect on the overall strength of the bonding structure. Xu and Wei [17] also studied the effect of adhesive thickness on the local interface fracture and overall strength of metallic adhesive bonding structures. They proposed a theoretical and numerical method based on the cohesive interface models, where the failure strength is the function of the thickness and the toughness of the adhesive layers.

Although many experimental investigations have been implemented as those mentioned above, the obtained results are still limited and local. Especially, few of them consider the effect of adhesive intrinsic material parameters on the relations between the overall strength and adhesive thickness. Indeed, some parameters such as toughness and strain-hardening capacity can affect the failure strength of joints. However, the related conclusions have been proposed based on only theoretical and modeling conjecture, without validation by experiments. In order to address the deficiency, in the present investigation, inspired by the theoretical model proposed by Xu and Wei [17], the effect of adhesive thickness on the overall strength of the SLJ was experimentally studied, considering the effect of toughness of the adhesive. The present experimental results are compared with the theoretical results finally.

2. Brief review of theory

Cohesive zone model based on traction-separation laws are well suitable to describe the de-cohesion behavior in bonding structures. When the cohesive zone model is employed to simulate the adhesive layer, the progressive failure of the adhesive can be captured by three cohesive parameters, namely initial stiffness, total fracture energy, and separation strength. All of these parameters would be influenced by adhesive thickness. According to the theoretical approach proposed by Xu and Wei [17], the separation strength is the most significant parameter and can be expressed by the functions adhesive thickness and toughness ratio, given as

$$\frac{\hat{\sigma}}{\sigma_f} = \begin{cases} \sqrt{\frac{1+\eta\left(\frac{t}{t_c}\right)}{(1+\eta)\cdot\left(\frac{t}{t_c}\right)}} & (t < t_c) \\ 1 & (t \geqslant t_c) \end{cases} \tag{1}$$

where $\hat{\sigma}$ is the separation strength, σ_f is the bulk shear strength of the adhesive obtained by the shear test, t is the adhesive thickness, t_c is the critical value of adhesive thickness, and η is the toughness ratio to describe the toughness of the adhesive, which can be defined by

$$\eta = \frac{Ut_c}{\Gamma_0} = \frac{2}{3\pi}\frac{E}{1-\nu^2}\frac{U}{\sigma_s^2} \tag{2}$$

where U is plastic dissipation in the unit volume, E is Young's modulus, ν is Poisson's ratio, σ_s is yield stress, and t_c is written by Equation (3),

$$t_c = 2r_p^{\max} = \alpha\frac{2}{3\pi}\frac{E}{1-\nu^2}\frac{\Gamma_0}{\sigma_s^2} \tag{3}$$

where α is the coefficient and ranges between 1.25 and 5 according to Pardoen et al. [16], and 1.25 is selected in the present investigation. Here, $r_p^{\max}$ is the maximum length that scales the plastic dissipation zone in front of the crack tip, Γ_0 is the cohesive energy, E is Young's modulus, and ν is the Poisson ratio of the adhesive.

3. Experimental setup

In the present investigation, the experiment consists of two steps: the first one is the test for assessment of the adhesives including tensile and shear tests, followed by the test for the SLJ.

3.1. Tensile sample test

For the tensile sample test, two types of adhesives were selected: one is very brittle adhesive (Epoxy WD1001 produced by Shanghai Kangda Co., China) and the other is very ductile (Silicone rubber 704 produced by Jiangsu Nanda Co., China), which have different toughness.

It is well known that the toughness of silicone rubber (SR) is usually higher than that of epoxy (EP). In order to obtain the accurate values of the toughness ratio η of the adhesives in the present experiment, tensile test with the specimens of the adhesives is needed. Some molds were prepared for the purpose of making the dog-bone specimens for the adhesives. In order to remove the specimen easily, the surfaces of the molds were polished with sandpaper and smoothed with a lubricant. Three SR and EP specimens were, respectively, prepared. All the specimens were put into the incubator maintaining a temperature of 25 °C for 30 days. Before measuring the size of the gage segment, the specimens were checked to avoid the visible crack affecting the experimental result. The geometry of the dog-bone specimen is shown in Figure 1. All the SR specimens were tested in a standard tensile tester under a crosshead speed of 0.2 mm/min and the EP specimens with a crosshead speed of 0.1 mm/min. Therefore, the entire loading process is quasi-static. Contacting extensometers tend to interfere with the mechanical behavior of the adhesive, which should be avoided. The technique used in the present experiment is an optical method in which the displacements/strains are obtained by spatial correlation of image pairs acquired initially (non-deformed) through loading.

3.2. *Shear test*

According to the existing researches, the overall strength of the SLJ increases with the decrease of adhesive thickness. For the structure of the SLJ, the interfaces between the adhesive and the adherend have a remarkable influence on the overall strength of the structure. Compared to the shear strength of the adhesive, it is still unknown that whether the influence of the adhesive interface on the failure strength is positive or negative. In order to solve the issue mentioned above, the bulk shear strengths of the adhesives used in the present experiments should be known.

In order to obtain accurate values of the shear strength of the aforementioned adhesives, two methods (i.e. A and B) were designed in Figure 2:

(A) two-segment shear test;

(B) three-segment shear test.

It is worth noting that the number of fracture surfaces of the two methods is different, as shown in Figure 2. And the number is 1 and 2, respectively. The shear strength could be obtained as

$$\tau = \frac{F}{n \cdot A} \tag{4}$$

where F is the maximum load during the loading process, n is the number of the fracture surfaces, and A is the area of cross-section of the shear specimen. Two types of

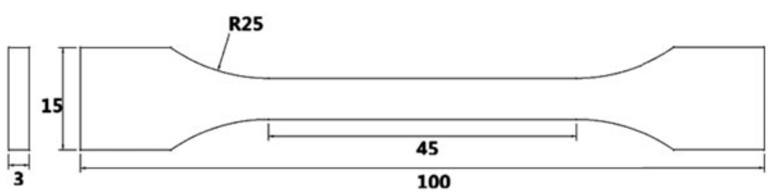

Figure 1. The geometry of the dog-bone specimen (unit: mm).

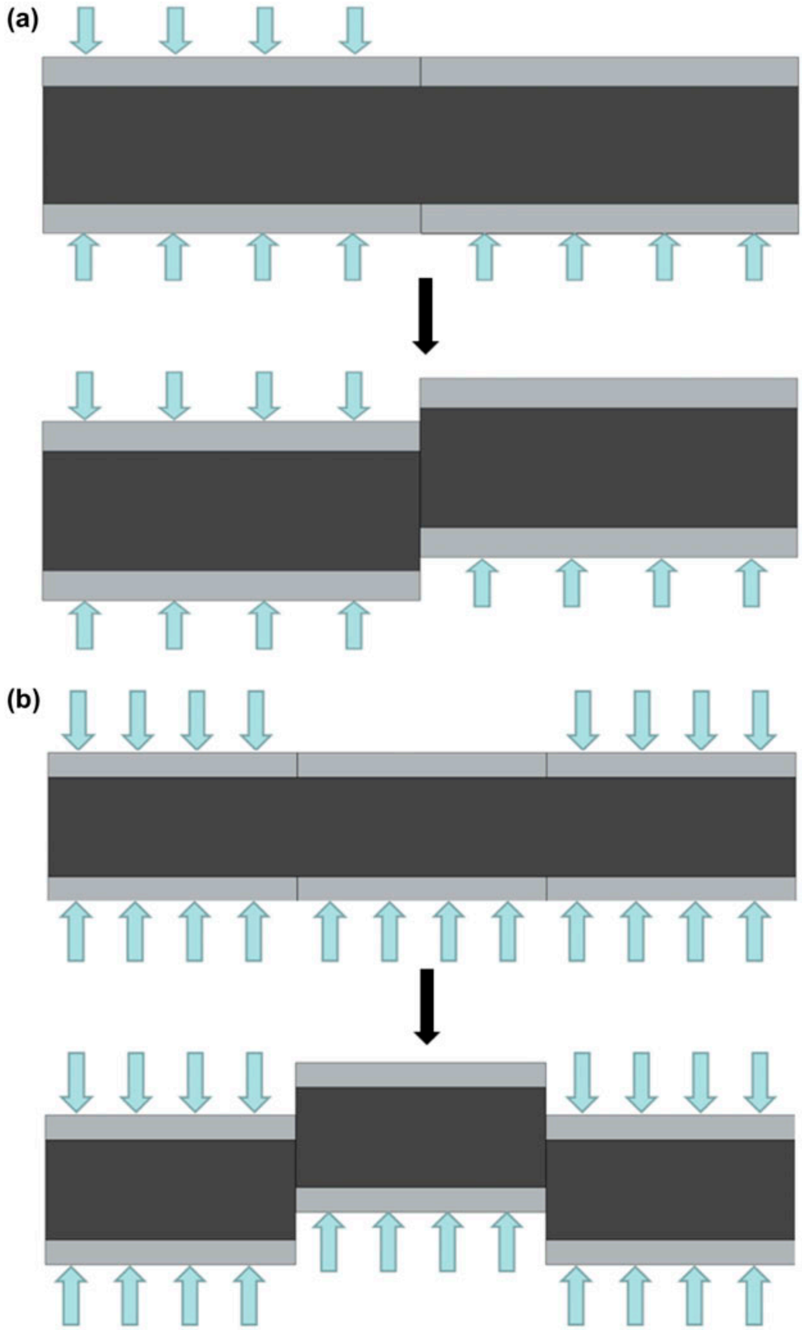

Figure 2. Two test methods to obtain the shear strength of the adhesive: (a) two-segment shear test (i.e. method A); (b) three-segment shear test (i.e. method B).

mold were prepared for the specimens. All the inner walls of the molds were pre-placed with a layer of greaseproof paper in order to easily remove the specimens from the molds after preliminary curing of the adhesives. All the specimens were placed in the thermostat with room temperature of approximately 25 °C for 30 days. It is worth mentioning that the process of curing of the liquid adhesive, especially the EP, was an exothermic reaction. In other words, the specimens suffered from thermal expansion and contraction during the whole curing process, which resulted in a rough surface of the specimen. Thus, the specimens were treated with sandpaper in order to eliminate the stress concentration before testing. The sectional dimensions of the specimens are shown in Table 1, where *b*, *l*, and *A* are the length, width, and area of the original cross-section of the specimens, respectively, and *A* is hence equal to $b \times l$. All the specimens were tested in a standard tensile tester under a crosshead speed of 0.2 mm/min as shown in Figure 3.

3.3. SLJ test

The geometry of the SLJ is shown in Figure 4, with a width of 25 mm and an overlap of 25 mm. The lightweight aluminum alloy 2024-T351 was selected here as the adherend material with a size of 120 × 25 × 3 mm. Before bonding, copper wires with various diameters were put on the bonding surface to control the adhesive thickness, as shown in Figure 5.

In order to improve the interface strength, the bonding surfaces of the aluminum alloy adherend should be properly pre-treated. The overlap of the adherend was successively polished with sandpaper with various granular diameters. Then, the ultrasonic cleaning machine was applied to clean up the surface of the adherend with alcohol for 5 min. The copper wires were cut into 25 mm length and put on both sides of the overlap of the adherend, as shown in Figure 5. A fast solidification glue (Ethyl cyanoacrylate) was used to fix the copper wire onto the adherend to prevent sliding during the process of gluing.

To precisely control the bonding area, the surface near the bond area was sprayed with a lubricant. In the present experimental investigation, 10 adhesive thickness were carried out for each type of adhesive. For the purpose of obtaining reliable results, three samples with identical presetting adhesive thickness were prepared for each type of adhesive. Therefore, as many as 60 specimens were prepared with specific numbers. Table 2 presents the number and the adhesive thickness of these specimens. All the specimens were put into the incubator which was maintained at the room temperature of 25 °C for 30 days to obtain full solidification. Before loading, the same materials used as adherends above were fixed at the end of all the specimens as shown in Figure 4. The purpose is to reduce the bending effect on experimental results. After full solidification, all the specimens were tested in a standard tensile tester at a crosshead speed of 0.2 mm/min.

Table 1. Geometry of the shear specimens.

Adhesive type	Specimen number	*b* (mm)	*l* (mm)	*A* (mm^2)	Method
Silicone rubber	1	10.30	9.72	100.12	A
	2	10.54	9.92	104.56	A
	3	11.00	10.00	110.00	B
	4	10.60	10.06	106.64	B
Epoxy	5	6.53	5.90	38.53	A
	6	6.08	6.55	39.82	A
	7	6.12	6.58	40.27	B
	8	6.34	6.29	39.87	B

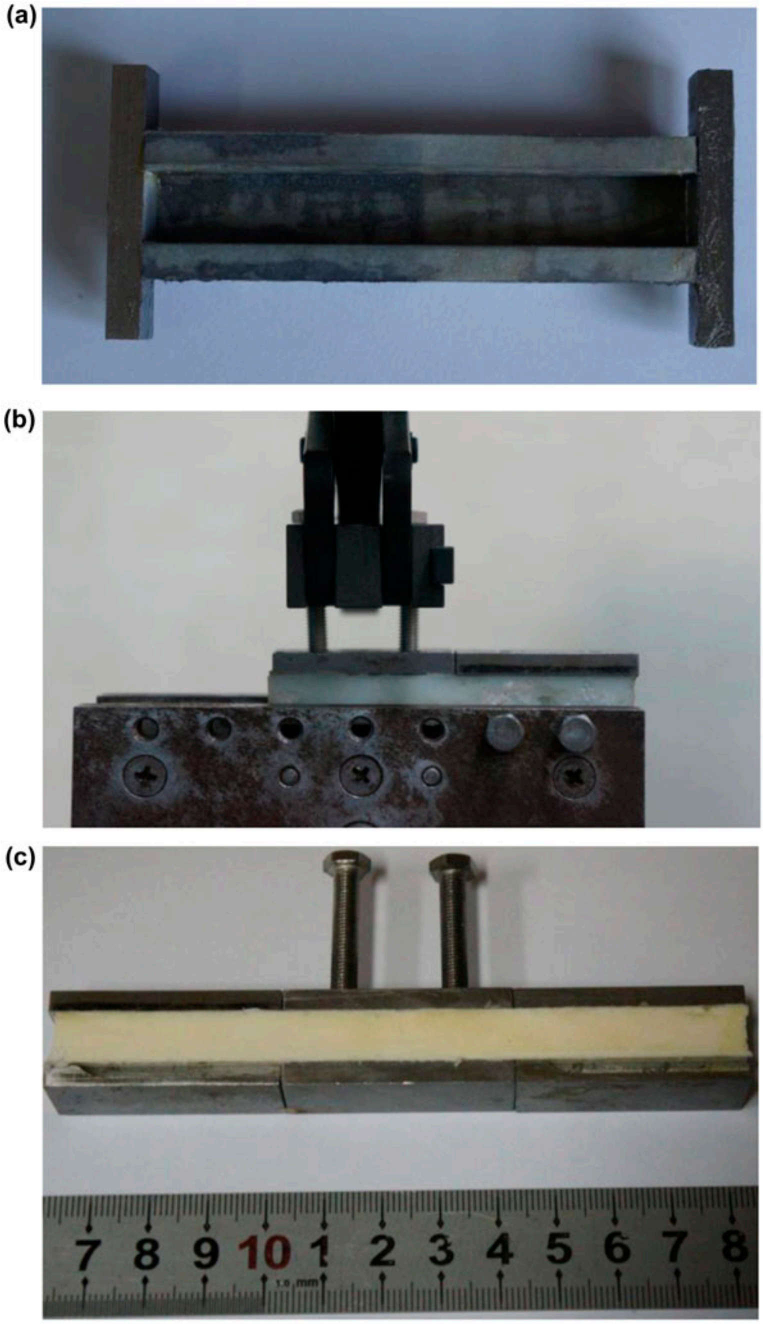

Figure 3. (a) Mold for the two-segment shear test; (b) experimental setup of two-segment shear test (i.e. method A); (c) experiment setup of three-segment shear test (i.e. method B).

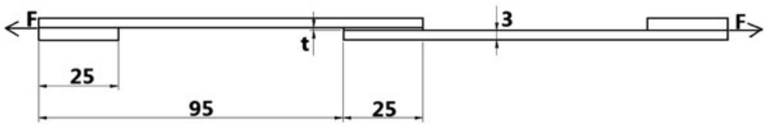

Figure 4. The single-lap joints' geometry (unit: mm and t is adhesive thickness).

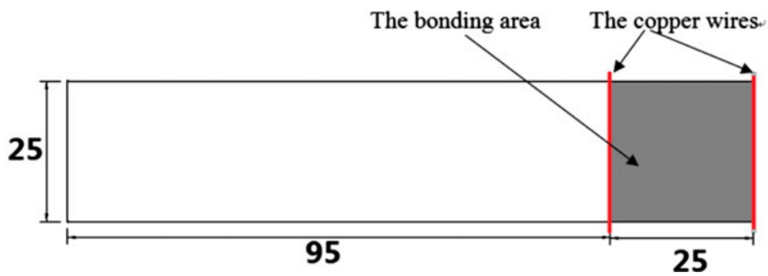

Figure 5. Copper wires bonded on adherend to control the adhesive thickness (unit: mm).

Table 2. Number and adhesive thickness of the specimens.

Specimen number	Adhesive thickness (mm)	Specimen number	Adhesive thickness (mm)	Specimen number	Adhesive thickness (mm)
SR-1	1.0	SR-21	1.0	SR-41	1.0
SR-2	0.8	SR-22	0.8	SR-42	0.8
SR-3	0.6	SR-23	0.6	SR-43	0.6
SR-4	0.5	SR-24	0.5	SR-44	0.5
SR-5	0.4	SR-25	0.4	SR-45	0.4
SR-6	0.3	SR-26	0.3	SR-46	0.3
SR-7	0.25	SR-27	0.25	SR-47	0.25
SR-8	0.2	SR-28	0.2	SR-48	0.2
SR-9	0.15	SR-29	0.15	SR-49	0.15
SR-10	0.02	SR-30	0.02	SR-50	0.02
EP-11	1.0	EP-31	1.0	EP-51	1.0
EP-12	0.8	EP-32	0.8	EP-52	0.8
EP-13	0.6	EP-33	0.6	EP-53	0.6
EP-14	0.5	EP-34	0.5	EP-54	0.5
EP-15	0.4	EP-35	0.4	EP-55	0.4
EP-16	0.3	EP-36	0.3	EP-56	0.3
EP-17	0.25	EP-37	0.25	EP-57	0.25
EP-18	0.2	EP-38	0.2	EP-58	0.2
EP-19	0.15	EP-39	0.15	EP-59	0.15
EP-20	0.02	EP-40	0.02	EP-60	0.02

4. Results and discussion

4.1. Tensile sample test

The stress–strain curves of the specimens were obtained and are shown in Figure 6. It can be observed that the dispersity of stress–strain curves for EP is larger than that for SR, because EP is more sensitive to defects and voids. Comparing Figure 6(a) with (b), the ultimate failure stress of EP is much higher than that of SR during the loading process. However, the corresponding failure strain is much smaller than that of SR. The yield strength was selected as equal to the stress value with a plastic strain of 0.2% in the stress–strain curves in Figure 6. According to the aforementioned method, Young's modulus E and yield strength σ_s can be calculated and are shown in Table 3. Compared with the whole area under stress–strain curve, the area under stress–strain curve with the strain from 0 to 0.2% is very small. Thus, the plastic dissipated energy in the unit volume U of the adhesive can be characterized by the area under the stress–strain curve as shown in Table 3. According to Equation (2), the toughness ratio of the adhesive

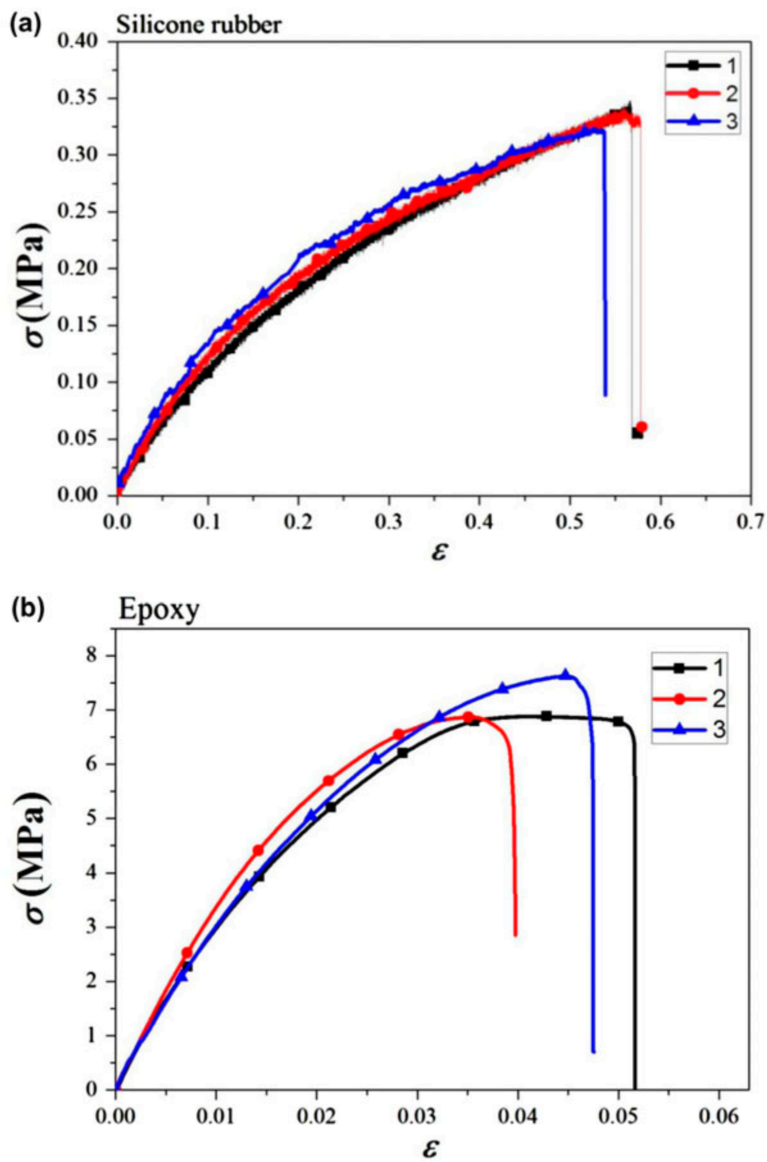

Figure 6. Stress–strain curves for the two types of adhesive tensile sample: (a) SR, (b) EP.

can be obtained and is given in Table 4. And the average of the toughness ratio of SR and EP is 26.04 and 2.33, respectively. The toughness ratio of EP is lower than that of SR. However, compared to the material parameters as given in Table 4, the Young's modulus E of EP and the yield stress σ_s of EP is 286.23 and 81.12 times larger than those of SR, respectively. As depicted in Equation (2), the square of the yield stress σ_s^2 of EP is 6561 times larger than SR's. In other words, σ_s^2 has a more prominent effect on the toughness ratio compared to the Young's modulus E, Poisson's ratio v, and the plastic dissipation in unit volume U.

4.2. Shear test

For the results of the shear test, the load–displacement curves by different test methods are shown in Figure 7. According to Equation (4) and the geometric dimensions of each specimen, as presented in Table 1, the shear strengths of the two adhesives are shown in Table 5. Comparing the experimental results by different methods, the discrepancy among the values of the shear strength for the same type of adhesive is slight. In other words, the experimental results are reliable.

4.3. SLJ test

During the loading process, all the specimens were cohesive failure. In other words, crack propagation occurred in the adhesive layer. After loading, each fracture surface of the specimens was checked to observe whether there were obvious defects and voids on them. The reason is that defects have a negative effect on the experimental results. Fortunately, no obvious defect was observed on the fracture surfaces. Under the quasi-static condition in the present experiments, each specimen has the corresponding load–displacement curves. The typical curves for the selected adhesive thickness are presented in Appendix 1. According to the load–displacement curves, the peak load and the corresponding displacement can be obtained, both of which change with the various adhesive thicknesses, as shown in Figure 8. The ultimate failure load increases as the adhesive thickness decreases as shown in Figure 8(a). Compared with the failure load, the relationship between the failure displacement and the adhesive thickness has

Table 3. Material parameters of the adhesives.

Type of adhesive		E (MPa)	σ_s (MPa)	v	U (J mm^{-2})	η	$\bar{\eta}$
Silicone rubber	1	1.33	0.0359	0.4	0.12	31.47	26.04 ± 6.7
	2	1.60	0.0433	0.4	0.13	27.36	
	3	1.60	0.0481	0.4	0.11	19.30	
Epoxy	1	380.68	2.9122	0.35	0.26	2.82	2.33 ± 0.7
	2	361.24	3.2889	0.35	0.20	1.61	
	3	371.31	2.9295	0.35	0.24	2.55	

Table 4. Ratio values of average material parameters for the two types of adhesives.

Material parameter	E	σ_s	v	U	η
$\frac{\text{Epoxy}}{\text{Silicone rubber}}$	286.23	81.12	0.88	2.15	0.09

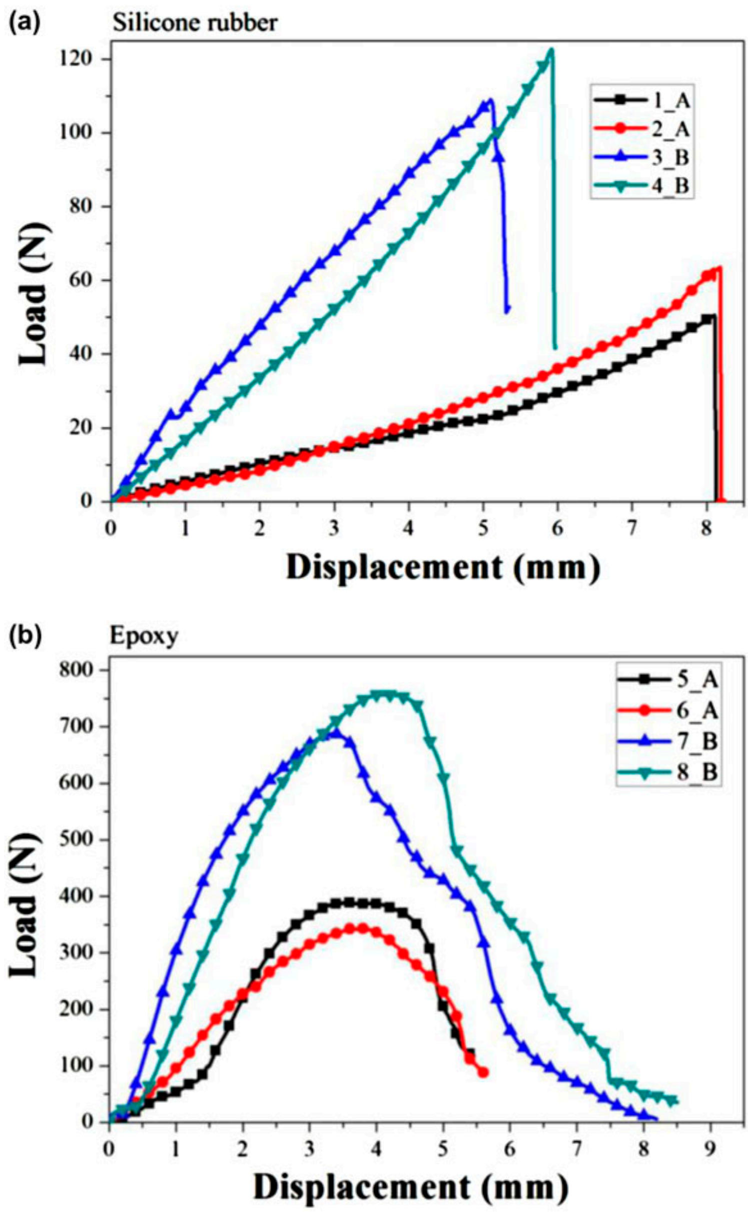

Figure 7. Load–displacement curves of the shear test with different methods and adhesives (A and B denote method A and B, respectively): (a) SR, (b) EP.

opposite tendency as shown in Figure 8(b). The same phenomenon occurs in the EP specimens as shown in Figure 8.

The peak stress corresponding to the ultimate failure load is given as,

$$\hat{\sigma} \approx \frac{F_P}{A_b} \tag{5}$$

Table 5. Shear strength of the adhesives.

Adhesive type	Specimen number	Shear strength (MPa)	Method	n	Average shear strength (MPa)
Silicone rubber	1	0.51	A	1	0.55 ± 0.04
	2	0.61	A	1	
	3	0.56	B	2	
	4	0.53	B	2	
Epoxy	5	10.12	A	1	9.19 ± 0.75
	6	8.62	A	1	
	7	8.54	B	2	
	8	9.50	B	2	

where $\widehat{\sigma}$ is the peak stress or the ultimate failure stress of the SLJ, F_P is the peak load, and A_b is the bonding area. In the present experiment, the bonding area of each specimen was 625 mm^2. According to Equation (5), the peak stresses $\widehat{\sigma}$ for all the specimens could be brought out and are shown in Figure 9. As expected, the peak stress increased as the adhesive thickness decreased for both the EP specimen and the SR specimen.

4.4. Further discussion

According to Ref. [16], the value of cohesive energy Γ_0 can be estimated by

$$\Gamma_0 \approx L \int_0^{0.2\%} \sigma d\varepsilon \tag{6}$$

where L is the gage length of the tensile specimens of the adhesives. According to Equation (6), Γ_0 can be estimated by the gage length and the area of stress–strain curve for the bulk sample in the standard sample test on the condition of $\varepsilon \leqslant 0.2\%$. According to Equations (3) and (6), t_c for the SR and the EP are 3.5 and 0.4 mm, respectively. Thus, the ratio of t_c between the SR and the EP is about 8.7.

In the SLJ test, the bonding area of all the specimens is 625 mm^2. And according to Equation (5), the ultimate failure strength with the variation of adhesive thickness is shown in Figure 9. What is worth noting is that the ultimate failure strength is almost unchanged with the increasing of adhesive thickness when the thickness exceeds a particular value (i.e. 0.4 mm) for EP. Then, the ultimate failure strength is stable at about 10 MPa, which is close to the average bulk shear strength of 9.2 MPa obtained in the shear test for EP. According to Equation (1), the strength ratio of the adhesive $\widehat{\sigma}/\sigma_f$ is a function of thickness ratio t/t_c, which is shown in Figure 10.

With the decrease of t/t_c for EP, $\widehat{\sigma}/\sigma_f$ tends to increase. When t/t_c is less than 1.0, $\widehat{\sigma}/\sigma_f$ is sensitive to the change of t/t_c. When t/t_c is larger than 1.0, the value of $\widehat{\sigma}/\sigma_f$ is almost unchanged and tends to be 1.0. In other words, when the adhesive thickness is less than the critical value of the adhesive thickness, the ultimate failure strength is larger than the bulk shear strength of the adhesive. The smaller the adhesive thickness, the larger the value of $\widehat{\sigma}/\sigma_f$. When the adhesive thickness exceeds the critical value of adhesive thickness, the failure strength is equal to the bulk shear strength of the adhesive. A similar phenomenon could be also found on adhesive joints with SR. Comparing the experimental results with the theoretical model prediction as shown in Figure 10, overall, the present experimental results agree with the theoretical model prediction except the range where the t/t_c is around 0.5.

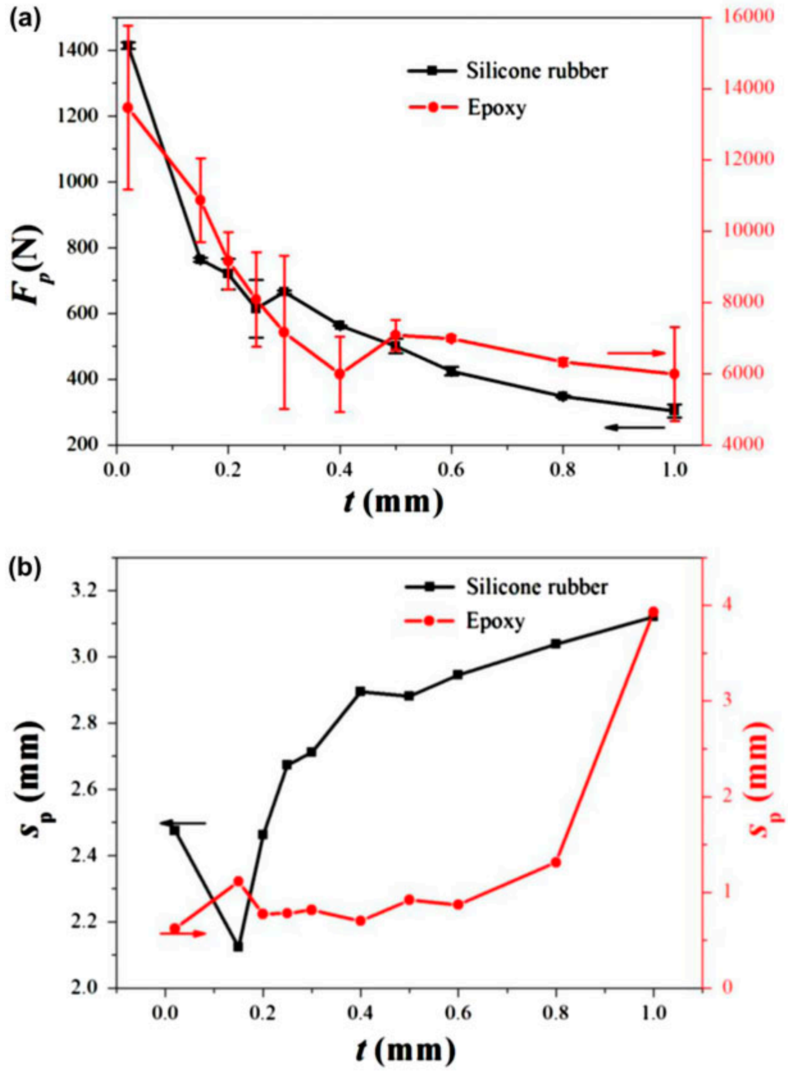

Figure 8. (a) Peak load and (b) critical displacement plotted as a function of various adhesive thicknesses.

It can be depicted by Figure 11 that when the adhesive thickness is less than t_c, the crack tip plastic dissipation zone is constrained by interfaces between the adhesive and the adherend as shown in Figure 11(a). And the ultimate failure strength is larger than the bulk shear strength of the adhesive. The larger the difference between t and t_c, the more the obvious restriction resulting from the interfaces between the adhesive and the adherend. It is similar to placing a thick pipe into a thin tube. When the adhesive thickness is equal to $t_c = 2r_p^{\max}$, the plastic dissipation zone is constrained by the upper and lower metallic adherends as shown in Figure 11(b). When the adhesive thickness exceeds t_c, crack propagation is entirely in the adhesive layer as shown in Figure 11(c). As a result, the interfaces do not restrict crack propagation any longer. Then, the

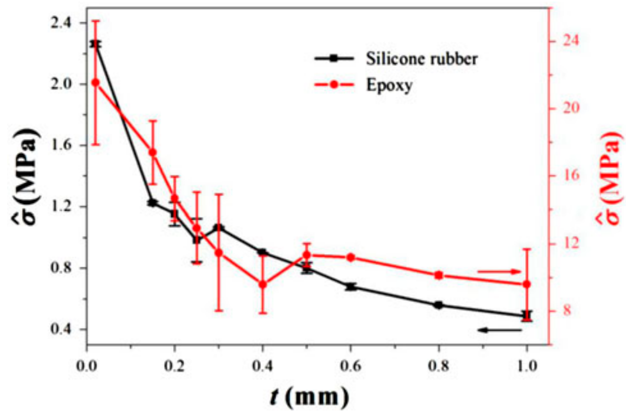

Figure 9. Ultimate failure strength plotted as a function of various adhesive thicknesses.

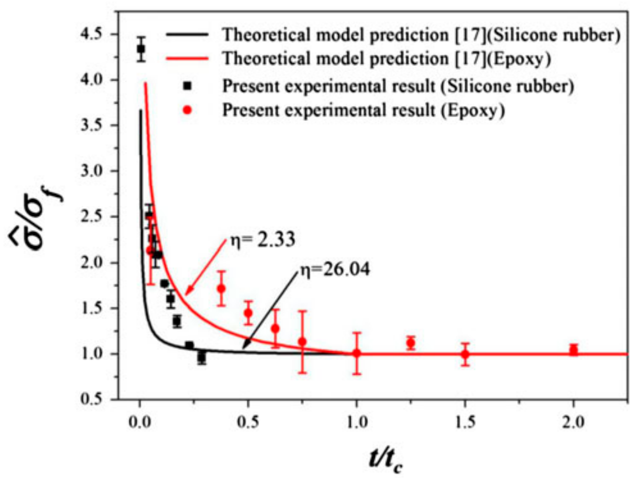

Figure 10. Normalized ultimate failure strength plotted as a function of the normalized adhesive thickness for SR and EP: comparison between the present experimental results with theoretical model prediction.[17]

ultimate failure strength is equal to the bulk shear strength of the adhesive. However, this is an ideal case. The real crack propagation path is not always in the mid-line of the adhesive layer, which can be explained the discrepancy between the computational values and experimental values as shown in Figure 10.

The average toughness ratio η of SR and EP is 26.04 and 2.33, respectively. On the condition of identical adhesive thickness, the toughness ratio η has a remarkable effect on the variation of the failure strength of the adhesive joints. When the adhesive thickness is less than t_c, the variation of the ultimate failure strength is sharper with the variation of the adhesive thickness for the relatively smaller adhesive toughness ratio (i.e. EP).

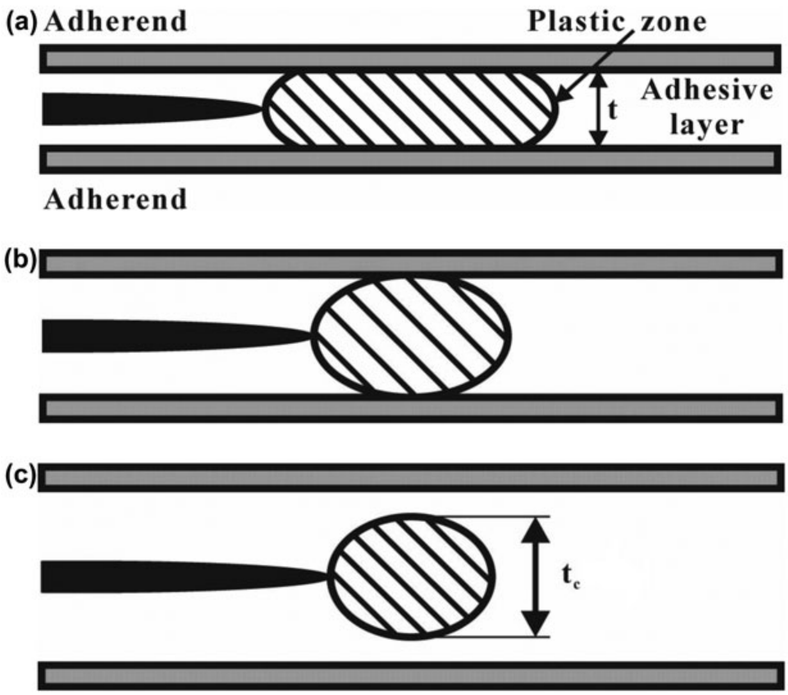

Figure 11. The relation between the plastic dissipation zone in front of crack tip and the adhesive thickness t, considering various adhesive thicknesses: (a) $t < t_c$; (b) $t = t_c$; (c) $t > t_c$.

Accordingly, the toughness ratio η can be regarded as a significant material parameter to describe the toughness of the adhesive, and the parameter is independent of adhesive thickness.

5. Conclusions

In summary, the effects of the toughness and thickness of adhesive layer are investigated by experiments. They have a combined effect on the ultimate failure strength of the metallic adhesive joints. The main conclusions can be drawn as follows:

When the adhesive thickness is smaller than the critical value, the ultimate failure strength of adhesive joints would increase with the decrease of adhesive thickness. The variation of the ultimate failure strength is more remarkable when the thickness is in the comparatively small thickness range. When the adhesive thickness is larger than the critical thickness, the failure strength tends to be a stable value, which is equal to the bulk shear strength of adhesive. Furthermore, the toughness ratio is also an intrinsic material parameter of the adhesive, when the adhesive thickness is smaller than the critical thickness, the variation of the ultimate failure strength is sharper with the variation of the adhesive thickness for the smaller adhesive toughness ratio. Therefore, the failure strength of the bonding structures is affected by both the adhesive thickness and the toughness ratio, which is in agreement with the previous theoretical model prediction.

Acknowledgments

This work was supported by the National Basic Research Program of China (No. 2012CB937500), the National Natural Science Foundation of China (No. 11021262, 10932011, 11023001, 11372318 and 91216108), and by the China Postdoctoral Science Foundation funded project (No. 2013M540033).

References

[1] Xu W, Wei YG. Assessments for impact of adhesive properties: modeling strength of metallic single lap joints. J. Adhes. Sci. Technol. 2013;27:9–29.
[2] Naito K, Onta M, Kogo Y. The effect of adhesive thickness on tensile and shear strength of polyimide adhesive. Int. J. Adhes. Adhes. 2012;36:77–85.
[3] Chai H. The effects of bond thickness, rate and temperature on the deformation and fracture of structural adhesives under shear loading. Int. J. Fract. 2004;130:497–515.
[4] Madhusudhana KS, Narasimhan R. Experimental and numerical investigations of mixed mode crack growth resistance of a ductile adhesive joint. Eng. Fract. Mech. 2002;69:865–883.
[5] Kahraman R, Sunar M, Yilbas B. Influence of adhesive thickness and filler content on the mechanical performance of aluminum single-lap joints bonded with aluminum powder filled epoxy adhesive. J. Mater. Process. Technol. 2008;205:183–189.
[6] Carlberger T, Stigh U. Influence of layer thickness on cohesive properties of an epoxy-based adhesive – an experimental study. J. Adhes. 2010;86:816–835.
[7] Marzi S, Biel A, Stigh U. On experimental methods to investigate the effect of layer thickness on the fracture behavior of adhesively bonded joints. Int. J. Adhes. Adhes. 2011;31:840–850.
[8] Xu W, Wei YG. Strength and interface failure mechanism of adhesive joints. Int. J. Adhes. Adhes. 2012;34:80–92.
[9] Duan K, Hu XZ, Mai YW. Substrate constraint and adhesive thickness effects on fracture toughness of adhesive joints. J. Adhes. Sci. Technol. 2004;18:39–53.
[10] Adams RD, Comyn J, Wake WC. Structural adhesive joints in engineering. 2nd ed. London: Chapman and Hall; 1997.
[11] da Silva LFM, Rodrigues T, Figueiredo MAV, de Moura M, Chousal JAG. Effect of adhesive type and thickness on the lap shear strength. J. Adhes. 2006;82:1091–1115.
[12] da Silva LFM, Critchlow GW, Figueiredo MAV. Parametric study of adhesively bonded single lap joints by the Taguchi method. J. Adhes. Sci. Technol. 2008;22:1477–1494.
[13] Lee DB, Ikeda T, Miyazaki N, Choi NS. Effect of bond thickness on the fracture toughness of adhesive joints. J. Eng. Mater. Technol. 2004;126:14–18.
[14] Castagnetti D, Spaggiari A, Dragoni E. Effect of bondline thickness on the static strength of structural adhesives under nearly-homogeneous shear stresses. J. Adhes. 2011;87:780–803.
[15] Gleich DM, Van Tooren MJL, Beukers A. Analysis and evaluation of bondline thickness effects on failure load in adhesively bonded structures. J. Adhes. Sci. Technol. 2001;15:1091–1101.
[16] Pardoen T, Ferracin T, Landis CM, Delannay F. Constraint effects in adhesive joint fracture. J. Mech. Phys. Solids. 2005;53:1951–1983.
[17] Xu W, Wei YG. Influence of adhesive thickness on local interface fracture and overall strength of metallic adhesive bonding structures. Int. J. Adhes. Adhes. 2013;40:158–167.

Appendix 1

In Section 4.3, the peak loads and the corresponding critical displacements were obtained for the underlying load–displacement relations of SLJ subjected to tensile loading. For each type of adhesive, there are three load–displacement curves for every adhesive thickness. Here, the typical curves for the selected adhesive thickness (i.e. 0.2 mm) are presented in Figure A1.

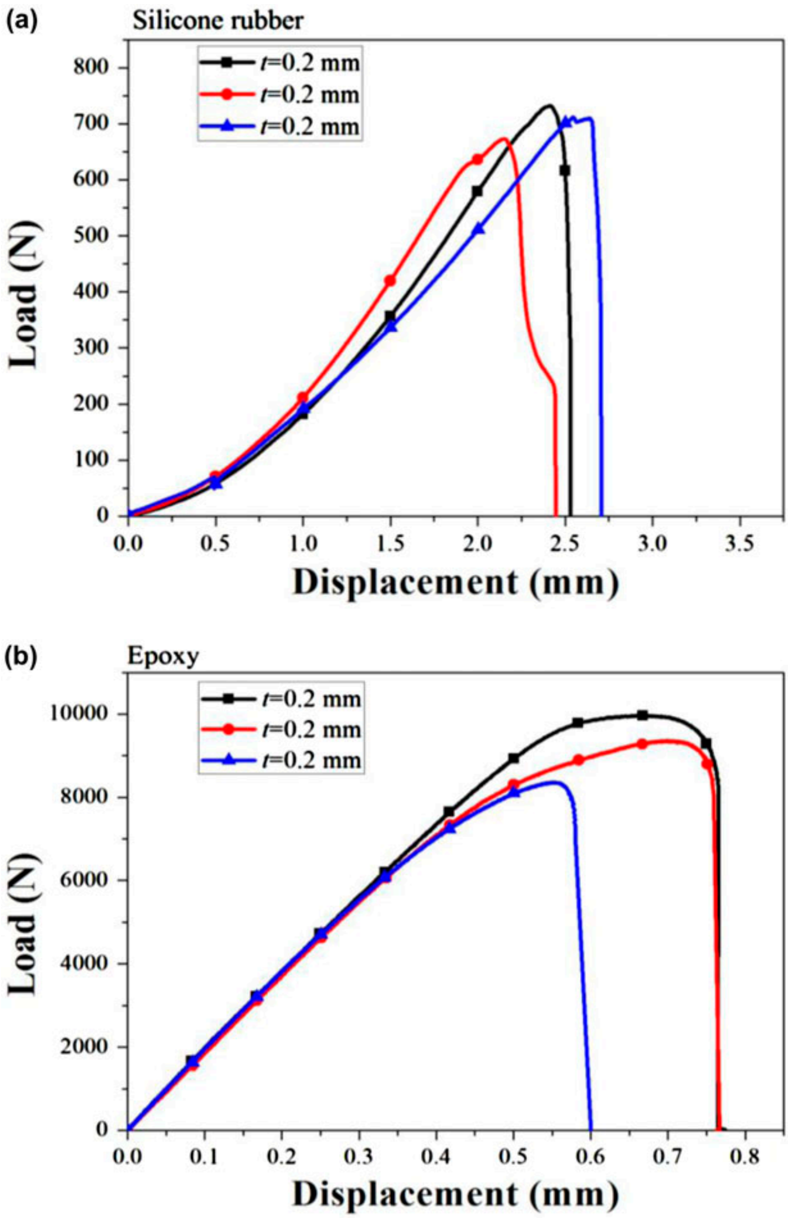

Figure A1. Load–displacement curves of the SLJ with the two types of adhesives for the selected adhesive thickness: (a) SR, (b) EP.